SUPPLEMENTARY MATERIALS:

Supplementary Appendix:

Regeneron Genetics Center Banner Author List and Contribution Statements

All authors/contributors are listed in alphabetical order.

RGC Management and Leadership Team

Goncalo Abecasis, Aris Baras, Michael Cantor, Giovanni Coppola, Andrew Deubler, Aris Economides, Luca A. Lotta, John D. Overton, Jeffrey G. Reid, Alan Shuldiner, Katia Karalis and Katherine Siminovitch

Contribution: All authors contributed to securing funding, study design and oversight. All authors reviewed the final version of the manuscript.

Sequencing and Lab Operations

Christina Beechert, Caitlin Forsythe, Erin D. Fuller, Zhenhua Gu, Michael Lattari, Alexander Lopez, John D. Overton, Thomas D. Schleicher, Maria Sotiropoulos Padilla, Louis Widom, Sarah E. Wolf, Manasi Pradhan, Kia Manoochehri, Ricardo H. Ulloa.

Contribution: C.B., C.F., A.L., and J.D.O. performed and are responsible for sample genotyping. C.B, C.F., E.D.F., M.L., M.S.P., L.W., S.E.W., A.L., and J.D.O. performed and are responsible for exome sequencing. T.D.S., Z.G., A.L., and J.D.O. conceived and are responsible for laboratory automation. M.S.P., K.M., R.U., and J.D.O are responsible for sample tracking and the library information management system.

Genome Informatics

Xiaodong Bai, Suganthi Balasubramanian, Boris Boutkov, Gisu Eom, Lukas Habegger, Alicia Hawes, Shareef Khalid, Olga Krasheninina, Rouel Lanche, Adam J. Mansfield, Evan K. Maxwell,

Mona Nafde, Sean O'Keeffe, Max Orelus, Razvan Panea, Tommy Polanco, Ayesha Rasool, Jeffrey G. Reid, William Salerno, Jeffrey C. Staples

Contribution: X.B., A.H., O.K., A.M., S.O., R.P., T.P., A.R., W.S. and J.G.R. performed and are responsible for the compute logistics, analysis and infrastructure needed to produce exome and genotype data. G.E., M.O., M.N. and J.G.R. provided compute infrastructure development and operational support. S.B., S.K., and J.G.R. provide variant and gene annotations and their functional interpretation of variants. E.M., J.S., R.L., B.B., A.B., L.H., J.G.R. conceived and are responsible for creating, developing, and deploying analysis platforms and computational methods for analyzing genomic data.

Clinical Informatics:

Nilanjana Banerjee, Michael Cantor, Dadong Li, Deepika Sharma, Ashish Yadav

Contribution: All authors contributed to the clinical informatics of the project

Translational and Analytical Genetics:

Joshua Backman, Darren Li

Contribution: All authors contributed to the analytical analysis of the project.

Research Program Management

Esteban Chen, Marcus B. Jones, Jason Mighty, Michelle G. LeBlanc and Lyndon J. Mitnaul

Contribution: All authors contributed to the management and coordination of all research activities, planning and execution. All authors contributed to the review process for the final version of the manuscript.

GHS DiscovEHR banner authors

Lance J. Adams, Jackie Blank, Dale Bodian, Derek Boris, Adam Buchanan, David J. Carey, Ryan D. Colonie, F. Daniel Davis, Dustin N. Hartzel, Melissa Kelly, H. Lester Kirchner, Joseph B. Leader, David H. Ledbetter, Ph.D., J. Neil Manus, Christa L. Martin, Raghu P. Metpally, Michelle Meyer, Tooraj Mirshahi, Matthew Oetjens, Thomas Nate Person, Christopher Still, Natasha Strande, Amy Sturm, Jen Wagner, Marc Williams

Estonia Biobank Banner Author List

Andres Metspalu, Mari Nelis, Reedik Mägi & Tõnu Esko

Supplementary Methods:

Glaucoma phenotype definition

GHS, SINAI: ICD-based glaucoma case definition in GHS and SINAI required an in-patient diagnosis or ≥ 2 outpatient diagnoses of ICD-10-H40 in the EHR. Individuals with only 1 outpatient diagnosis were excluded from the analysis. ICD-based controls for glaucoma were defined as individuals who were not cases or excluded *(50, 51)*.

UKB: Glaucoma ICD-based definitions of cases in UKB required one or more of the following: a) ≥ 1 diagnosis in inpatient Health Episode Statistics (HES) records, b) a cause-of-death diagnosis in death registry, c) ≥ 2 diagnoses in outpatient data (READ codes mapped to ICD10). Since we had self-reported diagnoses available for glaucoma in UKB, we combined ICD-based and self-reported glaucoma to define cases. Individuals were considered cases if they: identified 'glaucoma' from the eye problems or disorders list in the touchscreen questionnaire (UKB field ID: 6148) or, stated they had glaucoma in the verbal interview (UKB field ID: 20002) or were a case for ICD-10 H40 glaucoma. Normal controls for glaucoma in UKB were defined as individuals who did not report having glaucoma in the touchscreen (UKB field ID: 6148) or the verbal interview (UKB field ID: 20002), and were defined as controls for ICD-based glaucoma as described above.

POAAGG: A detailed description of criteria used to define glaucoma cases in POAAGG is provided elsewhere *(49)*. In brief, POAG cases were defined as having an open iridocorneal angle and characteristic glaucomatous optic nerve findings in one or both eyes, characteristic visual field defects and all secondary causes of glaucoma excluded. Controls in POAAGG were defined as subjects older than 35, without high myopia (greater than -8.00 diopters) or presbyopia (+8.00 diopters), a family history of POAG, abnormal visual field, IOP greater than 21 mmHg,

neuroretinal rim thinning, excavation, notching or nerve fiber layer defects, optic nerves asymmetry or a cup to disc ratio between eyes greater than 0.2. Additional controls for POAAGG were identified from the Penn Medicine Biobank as individuals without ICD-9 diagnoses for glaucoma.

MALMO: Glaucoma cases were defined as individuals with ≥ 1 in-patient and ≥ 2 outpatient diagnoses for ICD8: 375, ICD9: 365 or ICD10: H40. Individuals with only 1 outpatient diagnosis were excluded from the analysis. Controls were individuals who were not cases or excluded.

EstBB: Glaucoma cases were defined as individuals with at least 2 records of ICD-10 H40 (and its descendants) and controls were individuals that without a diagnosis for ICD-10 H40-H42, ICD-10 H44.5 and ICD-10 Q15.0. Individuals with only 1 ICD-10 H40 code were excluded from the analysis.

HUNT: Glaucoma cases were defined as individuals with an ICD-10 H40 or an ICD-9 365 diagnosis code at 2 separate outpatient encounters or 1 in-patient encounter. Individuals with only 1 outpatient encounter were excluded from the analysis. Individuals were excluded from controls if they had any of the following codes: ICD-10 H40-H42, ICD-10 H44.51, ICD-10 Q15.0 / ICD-9 365, ICD-9 377.14 or ICD-9 360.42.

CGPS-CCHS: Diagnoses of glaucoma were collected from the national Danish Patient Registry from January 1st, 1977 to March 1st, 2018. The National Danish Patient Registry has information on all patient contacts with all clinical hospital departments in Denmark, including emergency wards and outpatient clinics (from 1994). Glaucoma cases were defined as individuals with ICD-10 H40 and/or ICD8 375, and controls were participants without any of these codes.

FinnGen: The FinnGen analysis used was finngen_r3_H7_GLAUCOMA. Glaucoma cases were defined as individuals with ICD-10 codes of H40-H42 in the electronic health records and controls were individuals without any of these codes.

Exome sequencing in UKB, GHS, MALMO and SINAI

High coverage whole-exome sequencing was performed at the Regeneron Genetics Center as previously described *(50, 51)*. NimbleGen probes (VCRome) or a modified version of the xGen design available from Integrated DNA Technologies (IDT) were used for target sequence capture. Sequencing was performed using 75-bp paired-end reads on Illumina v4 HiSeq 2500 or NovaSeq instruments. Sequencing had a coverage depth (ie, number of sequence-reads covering each nucleotide in the target areas of the genome) sufficient to provide greater than 20x coverage over 85% of targeted bases in 96% of VCRome samples and 20x coverage over 90% of targeted bases in 99% of IDT samples. Sequence read alignment and variant calling was based on the GRCh38 Human Genome reference sequence. Ensembl v85 gene definitions were used to determine the functional impact of single nucleotide variants and insertion-deletions. Predicted LOF genetic variants included (a) insertions or deletions resulting in a frameshift, (b) insertions, deletions or single nucleotide variants resulting in the introduction of a premature stop codon or in the loss of the transcription start site or stop site, and (c) variants in donor or acceptor splice sites. Missense variants were classified for likely functional impact according to the number of *in silico* prediction algorithms that predicted deleteriousness using SIFT *(58)*, Polyphen2_HDIV *(59)* and Polyphen2_HVAR *(59)*, LRT *(60)* and MutationTaster *(61)*. We aggregated rare variants for gene burden testing as previously described *(62)*. Briefly, rare variants were collapsed by gene region, such that individuals who are

125 homozygous reference for all variants are considered homozygous reference, heterozygous carriers
126 of any aggregated variant are considered heterozygous, and only minor allele homozygotes for an
127 aggregated variant are considered as minor allele homozygotes. Genotypes were not phased to
128 consider compound heterozygotes in burden testing. For each gene, we considered two categories
129 of masks: a strict burden of rare pLOFs and a more permissive burden of rare pLOFs and likely
130 deleterious missense variants. For each of these groups, we considered five separate burden masks
131 per gene, based on the frequency of the alternative allele of the variants that were screened in that
132 group: MAF ≤ 1%, MAF ≤ 0.1%, MAF ≤ 0.01%, MAF ≤ 0.001%, and singletons only. For the
133 purposes of gene burden testing, the singleton mask includes minor allele homozygotes if no other
134 variant carriers are observed in the dataset.
135
136 **Genotyping**
137 *UKB:* DNA samples were genotyped as described previously *(63)* using the Applied
138 Biosystems UK BiLEVE Axiom Array (N=49,950) or the closely related Applied Biosystems UK
139 Biobank Axiom Array (N=438,427). Genotype data for variants not included in the arrays were
140 inferred using three reference panels (Haplotype Reference Consortium, UK10K and 1000
141 Genomes Project phase 3) as described previously *(63)*.
142 *GHS, SINAI* and *MALMO*: For SINAI and MALMO, DNA from participants was
143 genotyped on the Global Screening Array (GSA) and for GHS, genotyping was done on either the
144 Illumina OmniExpress Exome (OMNI) or GSA. MALMO and SINAI were imputed to the HRC
145 reference panel using the University of Michigan Imputation Server. GHS was imputed to the
146 TOPMed reference panel (stratified by array) using the TOPMed Imputation Server. Prior to
147 imputation, we retained variants that had a MAF ≥ 0.1%, missingness < 1% and HWE $P > 10^{-15}$.

Following imputation for GHS, data from the OMNI and GSA datasets were merged for subsequent association analyses, which included an OMNI/GSA batch covariate, in addition to other covariates described below.

HUNT: The Trøndelag Health Study (HUNT) consists of four different population-based health surveys conducted in the county of Nord-Trøndelag, Norway over approximately 35 years (HUNT1 [1984-1986], HUNT2 [1995-1997], HUNT3 [2006-2008]), HUNT4 [2017-2019] *(45)*. At each survey, the entire adult population (≥ 20 years) was invited to participate by completing questionnaires, attending clinical examinations and interviews. Participation rates in HUNT1, HUNT2, HUNT3 and HUNT4 were 89.4%, 69.5% and 54.1%, 54.0%, respectively. Taken together, the study included more than 120,000 different individuals from Nord-Trøndelag County.

DNA from 71,860 HUNT samples was genotyped using Illumina HumanCoreExome arrays (HumanCoreExome12 v1.0, HumanCoreExome12 v1.1 and UM HUNT Biobank v1.0). Genotyping and quality control have been previously described *(64)*. Imputation was performed on samples of recent European ancestry using Minimac3 (v2.0.1, http://genome.sph.umich.edu/wiki/Minimac3) *(65)* and a merged reference panel that was constructed by combining the Haplotype Reference Consortium panel (release version 1.1) *(66)* and a local reference panel based on 2,202 whole-genome sequenced HUNT study participants.

EstBB: Genotyping of DNA samples from the Estonian Biobank was done at the Core Genotyping Lab of the Institute of Genomics, University of Tartu using the Illumina Global Screening Arrays (GSAv1.0, GSAv2.0, and GSAv2.0_EST). At the time of this study altogether 155,772 samples were genotyped and then PLINK format files were created using Illumina GenomeStudio v2.0.4. During the quality control all individuals with call-rate < 95% or mismatching sex that was defined based on the heterozygosity of X chromosome and sex in the

phenotype data, were excluded from the analysis. Variants were filtered by call-rate < 95% and HWE p-value < 1×10^{-4} (autosomal variants only). Variant positions were updated to Genome Reference Consortium Human Build 37 and all variants were changed to be from TOP strand using reference information provided by Dr. Will Rayner from the University of Oxford (https://www.well.ox.ac.uk/~wrayner/strand/). After QC the dataset contained 154,201 samples. Before imputation variants with MAF<1% and Indels were removed. Prephasing was done using the Eagle v2.3 software *(67)* (number of conditioning haplotypes Eagle2 uses when phasing each sample was set to: --Kpbwt=20000) and imputation was carried out using Beagle v.28Sep18.793 *(68, 69)* with an effective population size ne = 20,000. As a reference, Estonian population specific imputation reference of 2,297 whole genome sequenced (WGS) samples was used *(70)*.

CGPS-CCHS: *ANGPTL7* Gln175His was genotyped with the Illumina HumanExome BeadChip (n=19,719), and Arg177* was genotyped by Taqman (n=113,604). All Arg177* heterozygotes were verified by Sanger sequencing.

FinnGen: Individuals in FinnGen were genotyped with Illumina and Affymetrix chip arrays (Illumina Inc., San Diego, and Thermo Fisher Scientific, Santa Clara, CA, USA). Imputation was performed using the population specific SISu v3 imputation reference panel of 3,777 whole genomes. Additional details on genotyping and imputation can be found at: https://finngen.gitbook.io/documentation/.

Genetic association analyses in UKB, GHS, SINAI and MALMO

Association analyses in each study were performed using the genome-wide linear (for IOP) or Firth logistic (for glaucoma) regression test implemented in REGENIE *(52)*. We included in step 1 of REGENIE (i.e. prediction of individual trait values based on the genetic data) directly

194 genotyped variants with a minor allele frequency (MAF) > 1%, < 10% missingness, Hardy-
195 Weinberg equilibrium test $P > 10^{-15}$ and linkage-disequilibrium (LD) pruning (1000 variant
196 windows, 100 variant sliding windows and $r^2 < 0.9$). The association model used in step 2 of
197 REGENIE included as covariates (i) age, age^2, sex, age-by-sex and age^2-by-sex; (ii) 10 ancestry-
198 informative principal components (PCs) derived from the analysis of a set of LD-pruned (50
199 variant windows, 5 variant sliding windows and $r^2 < 0.5$) common variants from the array (imputed
200 for the GHS study) data generated separately for each ancestry; (iii) an indicator for exome
201 sequencing batch (GHS: three batches; UKB: six IDT batches); and (iv) 20 PCs derived from the
202 analysis of exome variants with a MAF < 1% also generated separately for each ancestry.
203 Within each study, association analyses were performed separately for individuals of
204 African (AFR) and European (EUR) ancestry, when available. We determined continental
205 ancestries by projecting each sample onto reference principal components calculated from the
206 HapMap3 reference panel. Briefly, we merged our samples with HapMap3 samples and kept only
207 SNPs in common between the two datasets. We further excluded SNPs with MAF < 10%, genotype
208 missingness > 5% or Hardy-Weinberg Equilibrium test $P < 10^{-5}$. We calculated PCs for the
209 HapMap3 samples and projected each of our samples onto those PCs. To assign a continental
210 ancestry group to each non-HapMap3 sample, we trained a kernel density estimator (KDE) using
211 the HapMap3 PCs and used the KDEs to calculate the likelihood of a given sample belonging to
212 each of the five continental ancestry groups. When the likelihood for a given ancestry group was
213 > 0.3, the sample was assigned to that ancestry group. When two ancestry groups had a likelihood
214 > 0.3, we arbitrarily assigned AFR over EUR, Admixed American (AMR) over EUR, AMR over
215 East Asian (EAS), South Asian (SAS) over EUR, and AMR over AFR. Samples were excluded
216 from analysis if no ancestry likelihoods were > 0.3, or if more than three ancestry likelihoods were

217 > 0.3. Results were subsequently meta-analyzed across studies and ancestries using an inverse
218 variance-weighted fixed-effects meta-analysis.
219
220 **Genetic association analyses in HUNT, EstBB, CGPS-CCHS and FinnGen**
221 *HUNT:* Association analyses were conducted using SAIGE *(53)*. Models were adjusted for
222 birth year, birth year squared, sex, birth year-by-sex interaction, genotyping batch and four
223 principal components (PCs). PCs were computed using PLINK. Additionally, the analyses were
224 restricted to participants of European ancestry.
225 *EstBB*: We conducted the GWASes using the SAIGE software *(53)* with mixed-model
226 logistic regressions and adjusting the analyses for the first four principal components of the
227 genotype matrix, as well as for age, age squared and sex.
228 *CGPS-CCHS*: The associations between *ANGPTL7* genotype and glaucoma were tested
229 with logistic regression, adjusted for sex and age.
230 *FinnGen:* GWAS in FinnGen was conducted using the SAIGE software and adjusted for
231 sex, age, first 10 principal components and genotyping batch.
232
233 **Phenome-wide association analysis for ANGPTL7 pLOF and missense variants**
234 We undertook a phenome-wide analysis of the association of an aggregate of pLOF and
235 missense variants in ANGPTL7 with hundreds of continuous traits or disease outcomes in the GHS
236 and UKB studies. Results were available for 24,082 outcomes across the two cohorts. To control
237 for the number of statistical tests performed, associations were considered statistically significant
238 if the association p-value met a Bonferroni correction for 24,082 tests, that is $P < 2 \times 10^{-6}$
239 (corresponding to a p-value threshold of 0.05 divided by 24,082 statistical tests).

Continuous traits and disease outcomes were defined as described below. In the UKB study, for continuous traits, the values of biomarker, imaging variables or other continuous traits measured during one of the UKB visits or their averages within a given study visit or across study visits were used as outcomes. For binary disease outcomes, case status definition required one or more of the following criteria to apply (a) self-reported disease status or use of medication at digital questionnaire or interview with a trained nurse or (b) EHR of inpatient encounters from the UK National Health Service Hospital Episode Statistics database coded using the ICD-10 coding system. For each binary outcome, controls were individuals without any of the criteria for case definition. In the GHS study, for binary disease outcomes, case status definition required one or more of the following criteria to apply: (1) a problem-list entry of the ICD-10 diagnosis code, (2) an inpatient hospitalization-discharge ICD-10 diagnosis code, or (3) an encounter ICD-10 diagnosis code entered for 2 separate outpatient visits on separate calendar days. Controls were individuals without any of the criteria for case definition. Individuals were excluded if they had the relevant ICD-10 code associated with only one outpatient encounter. For continuous traits, data cleaning was performed by removing non-physiologic lab values, invalid or contaminated specimens, and those that were over 5 times the upper limit of normal. Then the minimum, median, and maximum laboratory result values over the duration of follow-up were derived for each patient and used as outcomes.

Small interfering RNA molecules

Small interfering RNAs molecules used in this study were synthesized by Alnylam Pharmaceuticals, Inc. (Cambridge, MA) as described by Nair et al *(71)*. The identities and purities of all oligonucleotides were confirmed by electrospray ionization mass spectroscopy and ion

exchange high-performance liquid chromatography, respectively. These are siRNA molecules that contain modified bases (2' mods) and such molecules are conjugated to a proprietary ocular targeting agent/moiety. Concentration of siRNA molecules used in this study were 15mg/ml.

Derivation of mean corneal refractive power and astigmatism from refractometry traits

Corneal refractive power and corneal astigmatism were derived from the autorefractometry and keratometry data available in UKB as previously described *(72)*. Briefly, corneal astigmatism was defined corneal power along strong meridian minus corneal power along weak meridian at 3mm diameter, whereas the corneal power was the average of these two values for each eye. Refractive astigmatism is defined as the mean cylindrical power between both eyes *(73)*.

Generation of *Angptl7*$^{-/-}$ mice

The genetically engineered *Angptl7*-/- mouse strain was created using Regeneron's VelociGene technology *(74, 75)*. Briefly, mouse embryonic stem cells (50% C57BL/6NTac; 50% 129S6/SvEvTac; and Crb1$^{+/+}$) were targeted for ablation of a 571 base pair region of the *Angptl7* locus, beginning 153 base pairs upstream of the start ATG (mm10 chr4:148,499,872-148,500,442). A self-deleting Hygromycin selection cassette was targeted to the deletion for selection in embryonic stem cells. Heterozygous targeted cells were microinjected into 8-cell embryos from Charles River Laboratories Swiss Webster albino mice, yielding F0 VelociMice that were 100% derived from the targeted cells *(75)*. These mice were subsequently bred to homozygosity and maintained in the Regeneron animal facility during the study period. The resistance cassette was removed during F0 breeding using self-deleting technology. All protocols were approved by the Institutional Animal Care and Use Committee in accordance with the Regeneron's Institutional

Animal Care and Use Committee (IACUC) and the Association for Research in Vision and Ophthalmology (ARVO) Statement for the Use of Animals in Ophthalmic and Vision Research.

Anterior segment imaging using optical coherence tomography

Mice were anesthetized with 0.1 mg/kg of a ketamine/xylazine mixture (12 mg/ml and 0.5 mg/ml, respectively) and one drop of topical proparacaine (0.05%, sterile) on the eyes. After a minute, proparacaine was wiped off of the eyes and images of anterior segment of mice were collected using the infrared (IR) and optical coherence tomography + IR (OCT+IR) options on the Heidelberg Spectralis machine. Following parameters were used to capture images: sensitivity (42), position (-0.00 mm), ART (6 frames), size of scan (large), width and height (15 degrees × 10 degrees), and number of sections (81) were the same for all OCT and OCT+IR images. In addition, we used the sclera option for capturing OCT+IR images of mouse eyes. After acquiring images, mice were put on a warming station and monitored until they were fully awake and exhibiting normal behavior. Corneal thickness was measured using the Heidelberg Eye Explorer (version 1.5.9.0) by three experts in mouse eye anatomy from OCT images of the center of the cornea (section 41/81 at zoom 800%). The measurements from all three individuals were collated in the final plot.

IOP measurements in mice

IOPs were measured in mice as previously described *(55–57)*. Briefly, mice were anesthetized and IOP was measured in both eyes using a TonoLab rebound tonometer (Colonial Medical Supply, Franconia, NH) before the start of Angptl7 injection and every day afterwards for six days. When testing *Angptl7* siRNAs, IOPs were measured in each eye before then start of

experiment and then every week until end of study. IOP measurements for both eyes were completed in 3–5 minutes.

Injection of Angptl7 protein and siRNA into mouse eyes

A 33-gauge needle with a glass microsyringe (5-uL volume; Hamilton Company) was used for injections of Angptl7 protein/siRNA into mice eyes. For intravitreal injections, the eye was proptosed, and the needle was inserted through the equatorial sclera and into the vitreous chamber at an angle of approximately 45 degrees, taking care to avoid touching the posterior part of the lens or the retina. Angptl7 protein (catalog# 4960-AN-025; R&D Systems, Minneapolis, MN) or siRNA (from Alnylam Pharmaceuticals, Supplementary Methods) or PBS (1uL) was injected into the vitreous over the course of 1 minute. The needle was then left in place for a further 45 seconds (to facilitate mixing), before being rapidly withdrawn. Before and during intracameral injections of Angptl7 protein, mice were anesthetized with isoflurane (2.5%) containing oxygen (0.8 L/min). For topical anesthesia, both eyes received one to two drops of 0.5% proparacaine HCl (Akorn, Inc.). Each eye was proptosed and the needle was inserted through the cornea just above the limbal region and into the anterior chamber at an angle parallel to the cornea, taking care to avoid touching the iris, anterior lens capsule epithelium, or corneal endothelium. Up to 1uL of Angptl7 protein or PBS was injected into each eye over a 30-second period before the needle was withdrawn. Only one injection was administered at day 0.

In vitro characterization

HEK293 cell line was cultured in DMEM media (4.5g/L D-Glucose, (+) L-Glutamine, (-) Sodium Phosphate, (-) Sodium Pyruvate supplemented with 10% FBS and 1% Penicillin-

Streptomycin-Glutamine (Invitrogen), at 37°C in a humidified atmosphere under 5% CO_2. The day before transfection, HEK293 cells were seeded in OptiMEM supplemented with 10% FBS. After 24 hours, the cells were transfected with FuGENE 6, and 10μg of pcDNA 3.1(+) encoding the following proteins: ANGPTL7 wild type, Gln175His, Arg177* and Trp188*. After 24 hours, the media was changed with 2% FBS OptiMEM. The following day, the cells were collected in RIPA buffer, supplemented with protease and phosphatase inhibitors (BRAND) or TRIzol reagent (Invitrogen) for protein and RNA analysis, respectively. The supernatants were transferred to an Eppendorf tube and immediately flash frozen for downstream protein analysis. Western blot analysis was performed using a rabbit polyclonal antibody against ANGPTL7 at 1:1,000 dilution (10396-1-AP ProteinTech), using standard procedures. ANGPTL7 was quantified by ELISA according to manufacturer's instructions (LS-F50425 Life Sciences). The cell lysates were diluted 1:1,000. The supernatants were diluted 1:10,000. The ELISA plate was read at 450nm via SpectraMax M4 plate reader (Molecular Devices).

Total RNA was extracted using TRIzol reagent (Invitrogen) and RNeasy kit (Qiagen) according to manufacturer's instructions and treated with RNase-free DNase I (Promega). cDNA was synthesized using Superscript VILO cDNA synthesis kit (Invitrogen). Taqman analysis was performed using TaqMan Fast Advanced Master Mix (Applied Biosystems) in a QuantStudio 6 Flex (Applied Biosystems) and commercially available primers and probes for ANGPTL7 (Hs00221727 - Applied Biosystems) and GAPDH (Hs02786624_g1 - Applied Biosystems).

In situ hybridization using *RNAscope*

The expression pattern of TM single cell cluster specific gene expression in the human donor eye was determined by in situ hybridization using RNAscope® according to manufacturer's

specifications (Advanced Cell Diagnostics). Briefly, 10% NBF fixed and paraffin embedded human donor eye cups were cut into 5 to 10µm sections and mounted on SUPERFROST® Plus glass slides. For RNAscope, slides were baked on slide warmer for 1 hour at 60°C and deparaffinized for 20 minutes. Tissue sections then underwent 10 minutes of Pretreat 1- RNAscope hydrogen peroxide treatment (ACD, 320037) at room temperature, followed by 20 minutes of boiling at 90°C in Pretreat 2- target retrieval treatment (ACD, 320043) in Oster Steamer (IHC World, LLC, Model 5709) and 30 minutes of Pretreat 3- RNAscope protease plus treatment (ACD, 320037) at 40°C in a HybEZ Oven (ACD, 310010). Tissue sections were then incubated with DNaseI for 10 minutes at 40°C to reduce potential background from probes binding to genomic DNA. Tissue sections were then washed five times with water, hybridized with RNAscope probes for 2 hours at 40°C and the remainder of the manufacturer's assay protocol was implemented (ACD, 322360) from Amplified 1 to Amplified 6. The slides were washed twice (two minutes each at room temperature) with RNAscope wash buffer (ACD, 310091). Signal was detected by incubation with Red working solution (1:60 ratio of Red B to Red A) at room temperature for 10 minutes in the absence of light, followed by washing the slides in water several times and viewing under microscope. In some experiments, fluorescent signals were visualized and captured using an open-field Nikon Eclipse Ti-E microscope.

Table S1: Number of samples across cohorts included in IOP and glaucoma analyses.

S1A:

IOP (EUR)

Cohort	Data Type	# Samples
UKB	Array	101,590
	Imputed	108,120
	Exome	101,678
GHS	Imputed	28,977
	Exome	27,529

S1B:

Glaucoma (EUR)

Cohort	Data Type	# Cases	# Controls
UKB	Array	11,494	373,246
	Imputed	12,377	400,978
	Exome	11,502	373,538
GHS	Imputed	8,032	114,171
	Exome	7,562	110,602
SINAI	Array	409	9,178
	Imputed	409	9,178
	Exome	409	9,178
MALMO	Array	2,395	26,062
	Imputed	2,395	26,062
	Exome	2,395	26,062
FinnGen(R3)	Array/Imputed	3,463	93,036
EstBB	Array/Imputed	7,629	128,075
HUNT	Array/Imputed	3,874	64,541
CGPS-CCHS	Taqman	1,863	111,741

S1C:

IOP (AFR)

Cohort	Data Type	# Samples
UKB	Array	4,132
	Imputed	4,405
	Exome	4,114
POAAGG	Array	3,282
	Imputed	3,282
	Exome	3,167

S1D:

Glaucoma (AFR)

Cohort	Data Type	# Cases	# Controls
UKB	Array	449	7,374
	Imputed	481	7,922
	Exome	448	7,328
SINAI	Array	1,261	10,270
	Imputed	1,261	10,270
	Exome	1,261	10,270
POAAGG	Array	3,590	4,184
	Imputed	3,590	4,184
	Exome	3,444	4,052

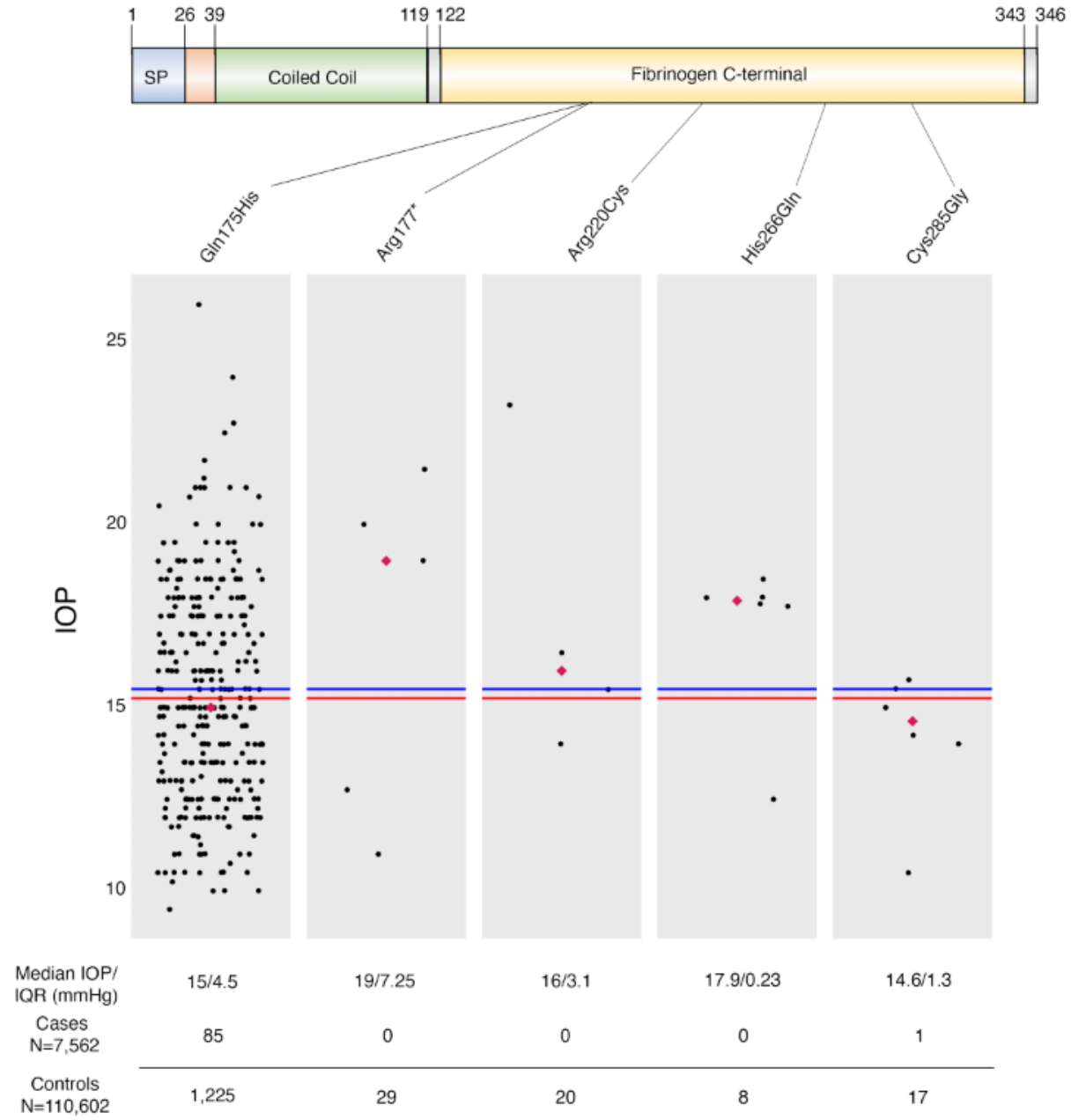

Figure S1: Missense and predicted loss-of-function (pLOF) variants in *ANGPTL7* and IOP levels in individuals of European descent in GHS. The plots represent Goldmann-correlated IOP (mean of both eyes) levels in carriers of 1 pLOF and 4 missense variants in *ANGPTL7* that are predicted deleterious by five different algorithms and have at least five carriers amongst the 27,529

exome-sequenced individuals with IOP measurements in GHS. The median IOP level across carriers of all 32 pLOF and predicted-deleterious missense *ANGPTL7* variants (15.25 mmHg) is indicated by the red line, and the median IOP in non-variant carriers (15.50 mmHg) is indicated by the blue line. Magenta diamonds mark the median IOP in carriers of each variant. Beneath the plots is the median and interquartile range of IOP and the numbers of variant carriers diagnosed with glaucoma or controls in GHS (n=118,164).

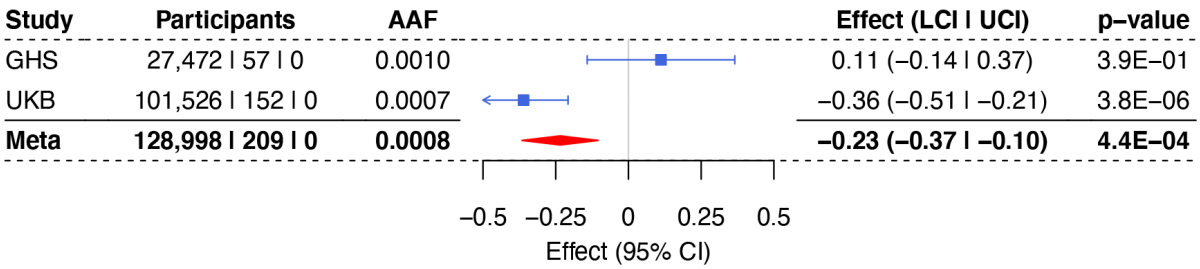

Figure S2: Meta-analysis of ANGPTL7 aggregate of predicted loss-of-function and deleterious missense variants (MAF < 1%), excluding Gln175His and Arg177*, with IOP. A total of 61 variants were present in the burden test.

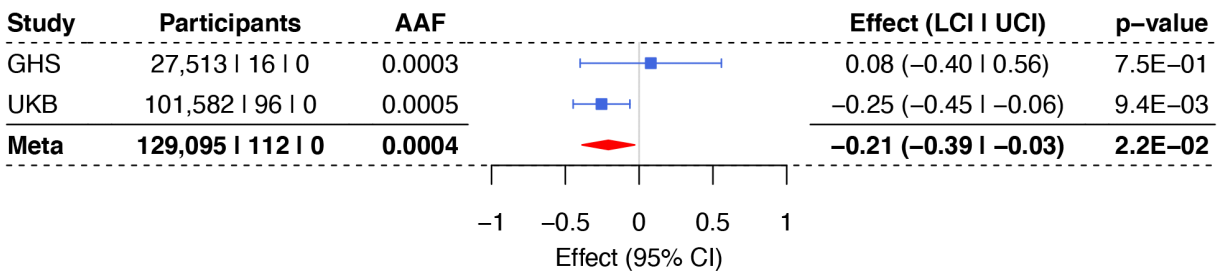

Figure S3: Meta-analysis of ANGPTL7 aggregate of predicted loss-of-function variants only (MAF<1%) with IOP. Arg177* is included in this aggregate of 15 variants.

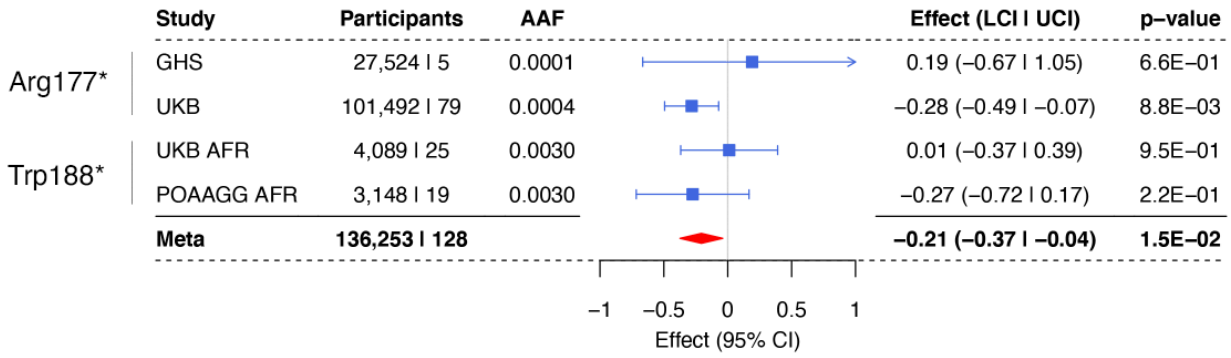

Figure S4: Cross-ancestry meta-analysis of Arg177* and Trp188* with IOP. AFR = African ancestry cohorts.

Table S2: Association of ANGPTL7 aggregate of pLOF and deleterious missense variants and ocular traits of interest in UKB.

Trait	P-value	Effect in SD (LCI | UCI)
CH (mean of both eyes)	7.50E-03	-0.06[-0.10 | -0.16
Moderate to low myopia (20262)	5.20E-02	1.1 [1.0 | 1.3]
ICD10 H52.1: Myopia	2.90E-01	1.2 [0.85 | 1.7]
High myopia (20262)	8.30E-01	0.97 [0.76 | 1.2]
Mean Spherical Equivalent (mean of both eyes)	1.40E-01	-0.032 [-0.074 | 0.010]
Corneal Astigmatism 6mm (left eye)	2.80E-01	-0.027 [-0.075 | 0.022]
Corneal Astigmatism 6mm (right eye)	5.80E-01	-0.014 [-0.062 | 0.035]
Corneal Astigmatism 3mm (left eye)	9.80E-01	0.00071 [-0.045 | 0.046]
Corneal Astigmatism 3mm (right eye)	1.00E+00	-0.00014 [-0.045 | 0.045]
Refractive Astigmatism	9.10E-01	0.0025 [-0.041 | 0.046]

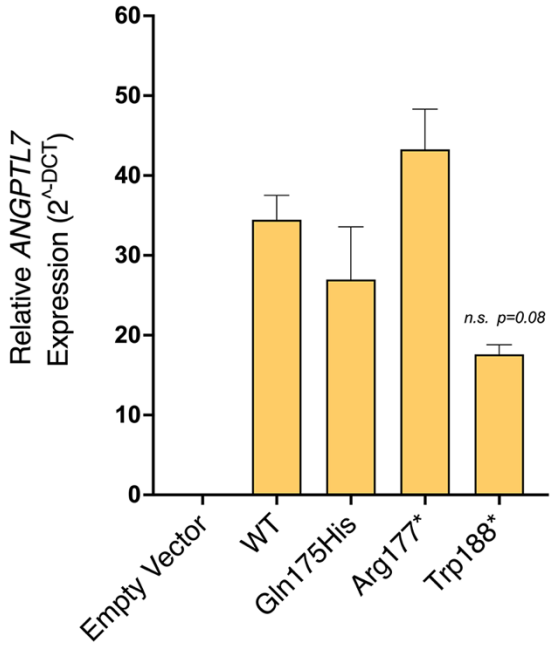

438

439 **Figure S5: Relative expression of WT and variant ANGPTL7 mRNA in a HEK293 cell line.**

440 qPCR shows mRNA levels of ANGPTL7 wild type, ANGPTL7 Gln175His, Arg177* and

441 Trp188*, after transfection in HEK293. The experiment shows the average expression of

442 ANGPTL7 and its variants in three biological replicates. Technical replicates (n=3) were run for

443 all three qPCR replicates. P-values were calculated by one-way ANOVA with Tukey's post hoc

444 analysis. Data are represented as mean ± SEM.

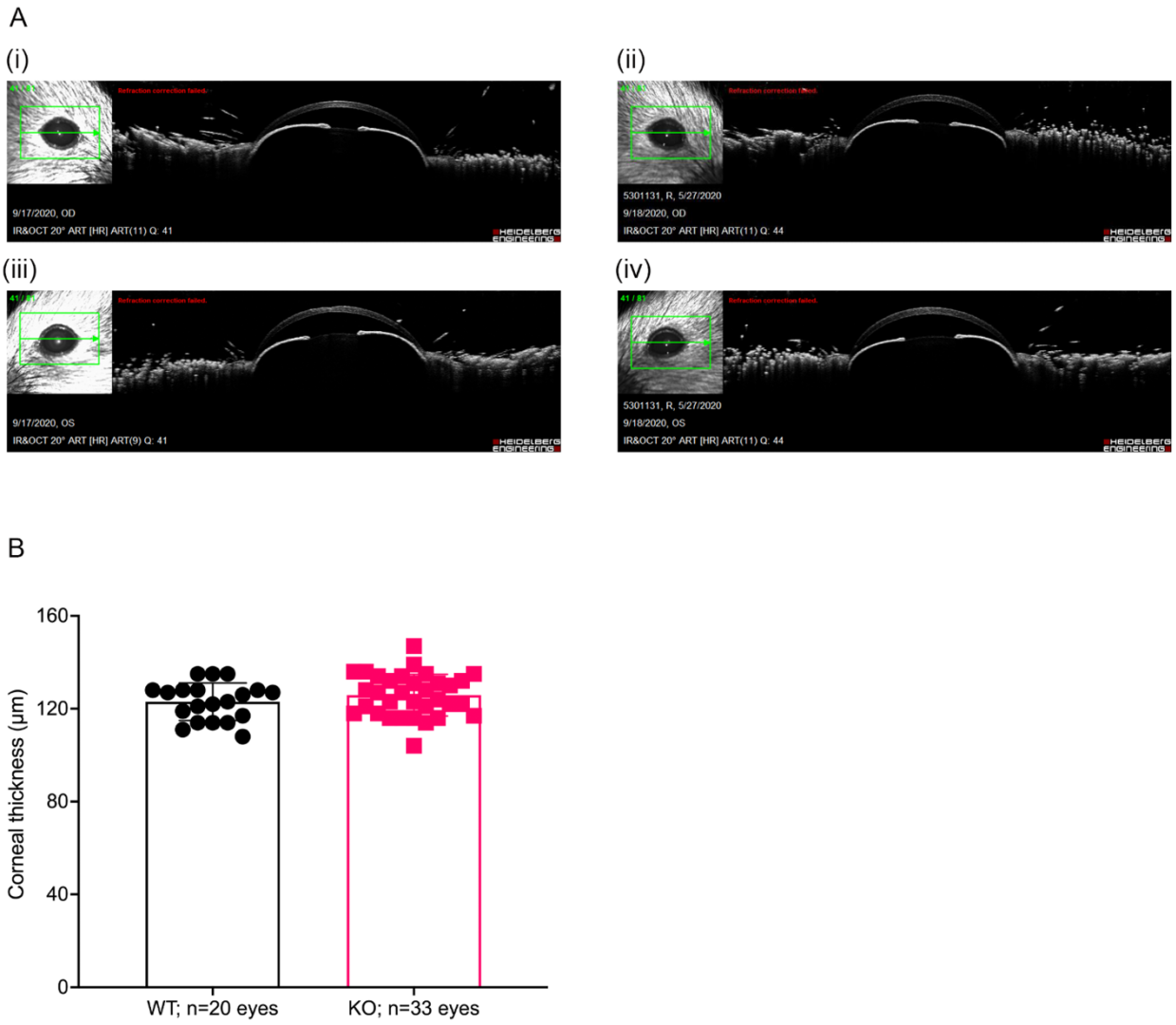

Figure S6: Characterization of Angptl7 KO and WT mouse eyes by OCT. (A) No ocular changes were observed between Angptl7 KO (ii, iv) and WT (i, iii) mouse eyes on anterior segment optical coherence tomography (OCT). **(B)** Angptl7 KO and WT mice had similar corneal thickness. Error bars represent the standard deviation.

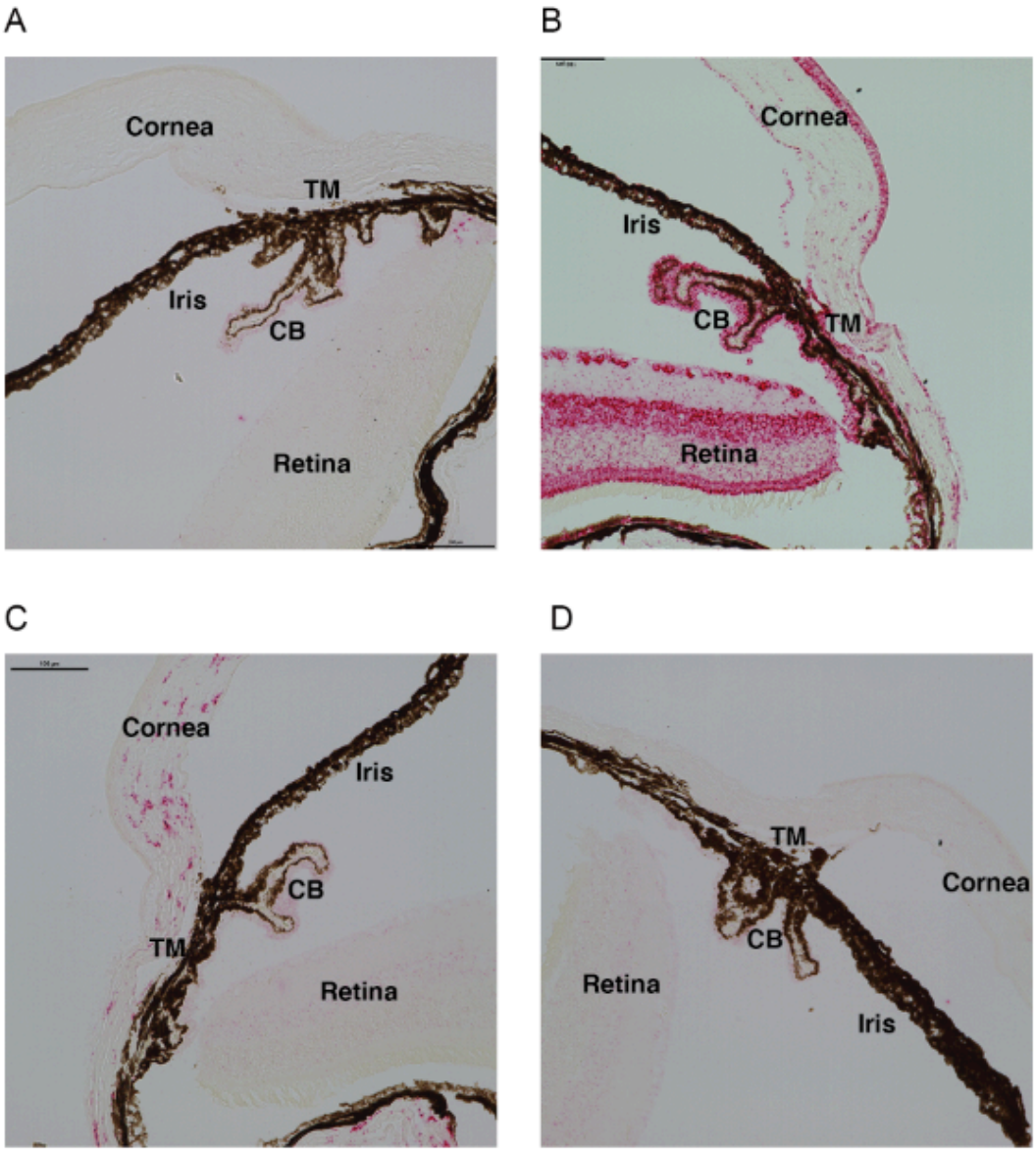

Figure S7: *In situ* characterization of Angptl7 mRNA in WT and *Angptl7* KO mouse eyes. Angptl7 mRNA was not expressed in any ocular tissue in *Angptl7* KO mice whereas it was expressed in TM, cornea, and sclera of WT mice as shown by *in situ* hybridization (RNAscope). Brightfield images showing following probes **(A)** Negative control- DapB, **(B)** Positive control- Ubc (red), **(C)** WT mice- Angptl7 (red), and **(D)** *Angptl7* KO mice- Angptl7 (no signal). Scale bar: 100 μm.